Tailored Bifunctional Polymer for Plutonium Monitoring

ARTICLE *in* ANALYTICAL CHEMISTRY · JUNE 2014

Impact Factor: 5.64 · DOI: 10.1021/ac501509t · Source: PubMed

5 AUTHORS, INCLUDING:

Sumana Chakraborty
Bhabha Atomic Research Centre
12 PUBLICATIONS **17** CITATIONS
SEE PROFILE

Ashok K Pandey
Bhabha Atomic Research Centre
106 PUBLICATIONS **1,234** CITATIONS
SEE PROFILE

Suresh Kumar Aggarwal
Homi Bhabha National Institute
251 PUBLICATIONS **1,404** CITATIONS
SEE PROFILE

analytical chemistry

Article

pubs.acs.org/ac

Tailored Bifunctional Polymer for Plutonium Monitoring

Sumana Paul,[†] Ashok K. Pandey,[‡] Pranaw Kumar,[†] Santu Kaity,[§] and Suresh K. Aggarwal*[,†]

[†]Fuel Chemistry Division, [‡]Radiochemistry Division, and [§]Radiometallurgy Division, Bhabha Atomic Research Centre (BARC), Trombay, Mumbai-400 085, India

Supporting Information

ABSTRACT: Monitoring of actinides with sophisticated conventional methods is affected by matrix interferences, spectral interferences, isobaric interferences, polyatomic interferences, and abundance sensitivity problems. To circumvent these limitations, a self-supported disk and membrane-supported bifunctional polymer were tailored in the present work for acidity-dependent selectivity toward Pu(IV). The bifunctional polymer was found to be better than the polymer containing either a phosphate group or a sulfonic acid group in terms of (i) higher Pu(IV) sorption efficiency at 3−4 mol L^{-1} HNO_3, (ii) selective preconcentration of Pu(IV) in the presence of a trivalent actinide such as Am(III), and (iii) preferential sorption of Pu(IV) in the presence of a large excess of U(VI). The bifunctional polymer was formed as a self-supported matrix by bulk polymerization and also as a 1−2 μm thin layer anchored on a microporous poly(ether sulfone) by surface grafting. The proportions of sulfonic acid and phosphate groups in both the self-supported disk and membrane-supported bifunctional polymer were found to be the same as expected from the mole proportions of monomers in polymerizing solutions used for syntheses. α radiography by a solid-state nuclear track detector indicated fairly homogeneous anchoring of the bifunctional polymer on the surface of the membrane. Pu(IV) preconcentrated on a single bifunctional bead was used for determination of the Pu isotopic composition by thermal ionization mass spectrometry. The membrane-supported bifunctional polymer was used for preconcentration and subsequent quantification of Pu(IV) by α spectrometry using the absolute efficiency at a fixed counting geometry. The analytical performance of the membrane-supported-bifunctional-polymer-based α spectrometry method was found to be highly reproducible for assay of Pu(IV) in a variety of complex samples.

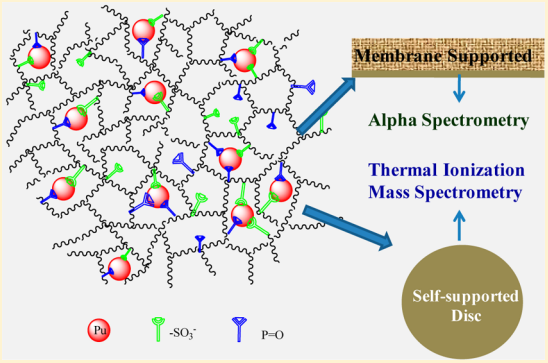

Various activities involved in the utilization of nuclear energy are potential sources of radiotoxic contamination of soil, natural waters, and biological systems.[1] The actinides are of major concern because of their high degree of radiological toxicity, though they might be present at ultratrace levels.[2] Precise and accurate determination of actinides is also required at different stages of the nuclear fuel cycle, i.e., input accountability of nuclear fuel, material accounting in the dissolver solution, burn-up determination, and recovery of precious actinides from radioactive waste, and most importantly for nuclear forensics. Recent events of the Fukushima−Daiichi accident highlighted the importance of developing a reliable analytical method for detection and quantification of plutonium in environmental samples.[3] In spite of continuous progress in the instrumental methods of analysis, pretreatment steps such as selective preconcentration of the analyte before its determination are frequently necessary to obtain a good signal and also to reduce the effect of interferences present in the matrix.[4] The instrumental methods used for quantification of actinides also have the problems of α energy overlap (α spectrometry), isobaric interferences (inductively coupled plasma mass spectrometry, ICPMS), polyatomic interferences (ICPMS), radiation selectivity (liquid scintillation counting), and abundance sensitivity interferences.[5] Therefore, a preconcentration step plays an exceptionally important role in the monitoring of actinides not only by enhancing the analytical range but also by providing chemical selectivity in the actinide detection methods. In addition, preconcentration makes it possible to manage the results without a large number of reference or standard samples because it provides concentration on a unified base.[6] During preconcentration, it is also possible to introduce internal standards.

The sorption preconcentration of actindes has been employed to develop combined and hybrid methods for the analyses of environmental and biological objects.[7−10] However, designing new sorbents with specified properties for quantitative recovery of elements from diverse objects remains a topical task.[11−14] Vajda and Kim have recently reviewed different analytical methodologies for quantification of transuranium isotopes (Pu, Np, Am) by radiometric techniques.[15] Ligands have been anchored on silica supports and superparamagnetic Fe_3O_4 particles for selective sequestration of actinides and fission products from aqueous media.[16−25] However, these materials are well suited for decontamination

Received: December 22, 2013
Accepted: June 5, 2014
Published: June 5, 2014

rather than for analytical applications. The commonly used separation methods for α spectrometry are coprecipitation, solvent extraction, ion exchange, and extraction chromatography using TEVA, TRU, and/or UTEVA resins.[26−28] Sequential extraction chromatography using TEVA, UTEVA, and DGA resin columns has been developed for the analyses of actinides sorbed in air filters using ICPMS.[29] For thermal ionization mass spectrometric analyses of Pu isotopes, a sample preparation sequence has been developed using column-based extraction chromatography followed by anion-exchange column separation.[30] However, these methods have multiple steps, and a small preconcentration factor is achieved. A new cloud point extraction procedure has been developed that can be coupled to either inductively coupled plasma mass spectrometry or α spectrometry for plutonium quantification.[31] An extraction chromatographic microflow system has been developed for automated determination of plutonium in a large volume of human urine.[32] However, it would be interesting to subject a solid-phase sorbent directly to conventional analytical techniques such as α spectrometry and thermal ionization mass spectrometry (TIMS) for quantification of the analyte preconcentrated in its matrix. This would minimize the sample manipulation steps for removal of the undesirable sample matrix without sacrificing the preconcentration factor.

In the present work, an extractive bifunctional polymer, having neutral phosphate and strong acidic sulfonic acid groups, has been developed for selective preconcentration of Pu(IV) and its subsequent analyses with TIMS and α spectrometry. The selection of a neutral phosphate group is based on the coordinating ability of the P═O moiety with actinide ions. The sulfonic acid groups have been incorporated into the bifunctional polymer for tuning the selectivity of P═O toward Pu(IV) and also for providing ion-exchange sites for charge balance. It has been observed by Alexandratos and Hussain that bifunctionality could enhance the complexation kinetics of the selective resins.[33] For comparing the improvement in the Pu(IV) preconcentration ability of the bifunctional polymer, monofunctional polymer disks containing either sulfonic acid or phosphate groups have also been prepared. The self-supported disks and membrane-supported bifunctional polymer have been synthesized using photoinduced free radical copolymerization and graft polymerization, respectively. The poly(ether sulfone) membrane has been selected for providing support as it is UV-active and suitable for surface grafting,[34] and also has a porous structure that would provide high accessibility of binding sites to the complexing ions. These materials have been characterized for chemical composition, physical structure, homogeneity, actinide sorption efficiency profiles as a function of HNO_3 concentration, sorption selectivity toward Pu(IV), and kinetics of Pu(IV) sorption and desorption from the polymer matrixes. The self-supported bifunctional disks/beads have been used for the removal of a matrix causing a high radiation field and for single-bead-based Pu(IV) loading in TIMS. The membrane-supported bifunctional polymer is ideal for ion-selective α spectrometry as it has a well-defined and reproducible geometry. Generally, the isotope dilution (ID) technique, which provides precise and accurate results as the method is independent of nonquantitative chemical recovery and matrix interference,[35] is employed for determination of the Pu concentration. However, Pu(IV) in the membrane samples has been quantified directly by α spectrometry due to the nearly constant Pu(IV) sorption efficiency and reproducible counting geometry (constant counting efficiency).

EXPERIMENTAL SECTION

Reagents and Apparatus. Analytical reagent grade chemicals, suprapure grade nitric acid (Merck, Mumbai, India), and deionized water (18 MΩ cm^{-1}) purified by Quantum from Millipore (Mumbai, India) were used throughout the studies. Poly(ether sulfone) (PES) membrane with a 0.1 μm pore size and 90 μm thickness from Pall Science was used. Phosphoric acid 2-hydroxyethyl methacrylate ester (HEMP) (containing 700−1000 ppm monomethyl ether hydroquinone, 90%), 2-acrylamido-2-methyl-1-propanesulfonic acid (AMPS), and α,α'-dimethoxy-α-phenylacetophenone (DMPA) were obtained from Sigma-Aldrich (Steinem, Switzerland). The chemical structures of the monomers used in preparing the bifunctional polymer are given in Figure S1 (Supporting Information). HEMP contains 25% diester, with the rest being in the triester form. Free radical bulk/graft polymerization of the monomers was carried out in a UV multilamp photoreactor procured from Heber Scientific, Chennai, India (model HML-SW-MW-LW-888) fitted with eight 8 W mercury UV lamps of 365 nm wavelength (Sankyo Denki, Japan) in a circle.

The stock solutions of U, Am, and Pu were obtained from the Mass Spectrometry Section, Fuel Chemistry Division, BARC, Mumbai, India. The specific α activity of Pu in the stock solution was determined to be 4.87 Bq pg^{-1} on the basis of its isotopic composition given in Table S1 (Supporting Information). A microprocessor-based pH meter, model PHAN, from Lab India (Mumbai, India) was used for the pH measurements. For determination of the α activity of actinides in aqueous solution, a 50 μL aliquot was added to a scintillation vial containing 5 mL of Ultima Gold AB scintillation cocktail (PerkinElmer). The α activity was measured with a home-built liquid scintillation counter. The γ activity measurement was carried out using an HPGe detector (ORTEC, United States) with a resolution of 550 eV (fwhm) at 122 keV coupled to a PC-based MCA. α spectra were recorded using the α spectrometer equipped with a passivated ion-implanted planar silicon (PIPS) detector (Canberra, PD-450-16-100AM) with an area of 450 mm^2 and a resolution of 16 keV (fwhm) at 5.486 MeV of ^{241}Am.

Syntheses of Bifunctional Polymers. The bifunctional disks were synthesized by the photoinduced free radical polymerization method as described in our earlier publications.[36] The appropriate amount of the UV initiator DMPA (1 wt %) was dissolved in a minimum volume of DMF, an equimolar mixture of HEMP and AMPS monomers in a mixed solvent containing a 1:1 (v/v) ratio of water and ethanol was added to it, and then the mixture was homogenized by ultrasonication for 5 min. The homogeneous mixture was poured into a circular Teflon mold with a 1 cm diameter, shown in Figure S2 (Supporting Information), and was irradiated with 365 nm light in a UV photoreactor for 15 min. The HEMP-*co*-AMPS polymer disks, obtained after irradiation, were washed with water at 70−80 °C to remove unpolymerized components and were conditioned by successive equilibrations with 0.5 mol L^{-1} NaOH and 0.5 mol L^{-1} HNO_3. After washing, the polymer was dried in an oven at 70−80 °C for 3−4 h and stored in 0.5 mol L^{-1} NaCl. A similar procedure was used to prepare the pure HEMP and AMPS polymer disks.

The PES host membrane undergoes UV-induced photolysis to form free radicals on polymer chains; see Figure S3

dx.doi.org/10.1021/ac501509t | Anal. Chem. 2014, 86, 6254−6261

(Supporting Information).[34] The free radicals formed on the surface of the PES membrane, exposed to UV light, were utilized to initiate the graft polymerization. Therefore, UV initiator DMPA was not used in the polymerizing solution. The monomers were grafted by irradiating 2 × 1 cm^2 pieces of the PES membrane, in contact with an equimolar mixture of HEMP and AMPS in a mixed solvent containing a 1:1 (v/v) ratio of water and ethanol, in the UV photoreactor for 15 min. The grafted membrane samples were washed and conditioned as described above for the polymer disks.

Characterization. The swelling ratio was determined from the weight (W_{wet}) of the water-equilibrated sample and dry weight (W_{dry}) of the same polymer sample:

$$\text{swelling ratio} = \frac{W_{wet}}{W_{dry}} \quad (1)$$

The porosity and effective surface area of the polymers (beads/disks) were measured using a mercury porosimeter. To study the chemical compositions, SEM−EDS (energy-dispersive spectroscopy) analyses were carried out to measure the phosphorus and sulfur contents at randomly selected surface points of both the polymer disk and membrane-supported polymer. The homogeneity of the binding sites on the PES membrane was studied by exposing the Pu-loaded sample to a CR-39 detector for recording the α tracks, developing the α tracks by chemical etching in 6 mol L^{-1} NaOH at 70 °C for 3.5 h,[37] and subjecting the α tracks to α radiography using an optical microscope (model BX-63, Olympus, Japan). The details of α radiography are given in our earlier publication.[10]

Sorption and Desorption Studies. To study the extraction properties of the polymers, about 100 mg of the polymer sample was equilibrated with 5 mL of well-stirred solution containing a tracer level concentration of Pu/Am. The amounts of actinides sorbed were monitored by γ-counting (^{241}Am) or α liquid scintillation counting (^{233}U and ^{239}Pu) of aqueous aliquots taken from the solution before and after equilibration with the polymer samples. The actinide sorption efficiency in the polymer samples was obtained from the following equation:

$$\text{sorption efficiency} = \frac{A_i - A_f}{A_i} \times 100 \quad (2)$$

where A_i and A_f are the radioactivities of actinide (α/γ count rate) in a solution before and after equilibration with the polymer sample, respectively. The $D_{Pu/U}$ values were obtained using the following equation:

$$D = \frac{A_0 - A_e}{W} \frac{V}{A_e} \quad (3)$$

where A_0 and A_e represent the radioactivities of ^{233}U/Pu initially and after equilibration in the aqueous phase, W and V are the weight of the solid phase (HEMP, AMPS, or HEMP-*co*-AMPS) and volume of the equilibrating aqueous phase, respectively. For studying the time required to obtain optimum sorption of actinides, about 200 mg of the polymer sample was added to 25 mL of aqueous solution containing trace levels of Pu(IV), and the solution was continuously stirred; a 10 μL aliquot was taken out at regular intervals from the equilibrating solution for monitoring the Pu activity.

Desorption of Am from the polymers was carried out using 3 mol L^{-1} HNO_3. For Pu, two separate stripping agents, viz., 0.1 mol L^{-1} HNO_3 and 1 mol L^{-1} $NH_2OH{\cdot}HCl$, were used. For desorption studies, about 100 mg of polymer sample was first equilibrated with 5 mL of aqueous solution containing a trace amount of actinide. After sorption of the actinide, the loaded polymer was filtered from the aqueous solution, washed with distilled water, and dried using filter papers. The filter paper was used to remove solution clinging on the surface of the polymer. The Pu-loaded polymer samples were then equilibrated with 5 mL of aqueous solution containing the appropriate concentration of the stripping agent.

Analytical Applications. The details of synthetic urine samples are described elsewhere.[10] The Pu activities in other environmental samples were spiked by drying appropriate volumes (25−100 μL) of Pu stock solution under IR lamps to near dryness and then adding known volumes (5−100 mL) of seawater and groundwater samples. Seawater and groundwater were collected from Trombay jetty, Mumbai and Kerala state, India, respectively.

The local soil samples were spiked with Pu activity by soaking them in very dilute Pu solution and evaporating to near dryness. The urine/seawater/groundwater samples were then treated with 3 mol L^{-1} HNO_3 to adjust the acidity and 20% H_2O_2 to convert Pu into Pu(IV). Pu was leached from the soil samples (2 g) by 100 mL of 8 mol L^{-1} HNO_3 containing 2−3 mL of 30% H_2O_2 with heating under an IR lamp. The HEMP-*co*-AMPS-grafted PES membranes with fixed dimensions (2 × 1 cm^2) were equilibrated with 5−30 mL volumes of treated aqueous samples for 1 and 24 h for a 100 mL volume under constant stirring at room temperature. After equilibration, the membranes were washed thoroughly with water, dried, and placed directly in front of an ion-implanted α detector to record the α spectra and obtain the α count rate at characteristic α energies (5.157−5.499 MeV) of ^{238,239,240}Pu isotopes. The Pu activity (Bq) in the membrane sample was obtained by correcting the measured α count rate with the absolute counting efficiency at a fixed counting geometry. The absolute α counting efficiency of the membrane sample with fixed dimensions was obtained by loading known activities of Pu(IV) in the membrane. For quantification of Pu in the aqueous sample, the Pu(IV) sorption efficiency of HEMP-*co*-AMPS was also taken into account.

For isotopic analyses by TIMS, PHWR (pressurized heavy water reactor) grade Pu (~1 μg) in 3 mol L^{-1} HNO_3 medium was equilibrated with a single bead of the HEMP-*co*-AMPS polymer for 1 h with continuous stirring. After equilibration, the bead was washed with 3 mol L^{-1} HNO_3, dried under an IR lamp, and loaded onto a high-purity rhenium filament for the TIMS analyses. All analyses were performed in the static mode of multicollection of the Isoprobe-T mass spectrometer using a double-filament assembly. Prior to the TIMS analyses, the filament was preheated from 0 to 2 A for 900 s, and degassing was carried out at 2 A for 1800 s. An about 300 mV signal was obtained for the $^{239}Pu^+$ ion when the vaporization filament heating current was 3 A; however, an optimum heating current of 3.6 A was chosen for plutonium isotopic analysis, at which an about 1 V $^{239}Pu^+$ signal current was produced. For comparison with the conventional solution loading method, the PHWR grade Pu samples were purified from U, Am, and other fission products using Dowex 1X8 resin.[38] Typically, the Pu sample was treated with H_2O_2 in 3 mol L^{-1} HNO_3 to convert Pu to Pu(IV), evaporated to near dryness, redissolved in 8 mol L^{-1} HNO_3, and loaded onto a ~5 cm Dowex 1X8 column. Am(III) and other fission products were eluted using 8 mol L^{-1} HNO_3,

dx.doi.org/10.1021/ac501509t | Anal. Chem. 2014, 86, 6254−6261

and U(VI) was eluted using 3 mol L^{-1} HNO_3. Pu(IV) was eluted using 0.3 mol L^{-1} HNO_3.

Safety Considerations. Low-level radioactive materials used in the present work were handled inside a fume hood connected to an exhaust system and using disposable latex gloves.

RESULTS AND DISCUSSION

Physical and Chemical Composition. The self-supported polymer disk is required to have a minimum change in dimensions with a sufficient porosity. The swelling ratio of the disk was found to be 1.3, which indicated the structural rigidity of the polymer. This may be attributed to the functional monomer HEMP having three polymerizable double bonds as shown in Figure S1a (Supporting Information), which would give rise to a high degree of cross-linking. The porosity and effective surface area were found to be 0.114 cm^3 g^{-1} and 34.33 m^2 g^{-1}, respectively, which are similar to those of other functional polymers reported elsewhere.[39] The SEM images indicated that the disk has a dense, lamellar structure with no visible micropores. The proportions of AMPS and HEMP were obtained by measuring the sulfur to phosphorus (S/P) ratio with an EDS analyzer; see Figure S4 (Supporting Information). The EDS analysis confirmed the homogeneous distribution of phosphate and sulfonic acid groups in the disk. There was reasonably good agreement of the experimental S/P ratio with that calculated for the bifunctional polymer disk based on the proportion of monomers used in the polymerizing solution, as given in Table 1. This indicated that the rates of polymerization of HEMP and AMPS monomers were equivalent, which can be attributed to the presence of a methacrylate moiety in both the monomers. However, the measured S/P ratio is representative of the statistical distribution of the two functional groups in the polymer, and does not mean the presence of alternate HEMP and AMPS units in a polymer chain. For analytical applications, it is essential to have a thin sorbent for preventing significant loss of α energy and a highly reproducible geometry for comparison with a standard. Therefore, the bifunctional polymer was grafted on the surface of the microporous PES membrane. As can be seen from Table 1, there is good agreement between the S/P ratio obtained from EDS analysis of the HEMP-*co*-AMPS-grafted PES membrane and that calculated from the proportion of monomers used in the polymerizing solution after correction for the S contribution from the host PES membrane. The distribution of S and P atoms on the surface of the PES membrane was found to be within ±2%.

Table 1. Elemental Analyses of the HEMP-*co*-AMPS Polymer Disk and HEMP-*co*-AMPS-Grafted PES Membrane by EDS

	concn, atom %		S/P ratio	
sample ID	S	P	measured	expected
HEMP-*co*-AMPS disk	56.2	43.8	1.28 ± 0.02	1.34
	56.6	43.4		
	55.7	44.3		
	56.0	43.9		
HEMP-*co*-AMPS-grafted PES membrane	58.2[a]	41.8	1.45 ± 0.03	1.47
	58.6[a]	41.4		
	59.9[a]	40.1		
	59.7[a]	40.3		

[a]Corrected for the contribution from the host PES membrane.

The FE-SEM image of the HEMP-*co*-AMPS-grafted PES membrane is shown in Figure 1a. The physical structure of the PES membrane did not change as the grafting yield was only 3 to 5 wt %. α track radiography was carried out using the Pu-loaded HEMP-*co*-AMPS-grafted membrane sample. It is seen from the micrograph given in Figure 1b that the α tracks were uniformly distributed. This could be correlated to the uniform distribution of binding sites on the surface of the HEMP-*co*-AMPS-grafted PES membrane. The microinhomogeneity of the α tracks could be attributed to pores as seen in the SEM image. To study the degradation of the α energy in the bifunctional polymer anchored on the surface of the PES membrane, the energy spectrum of α-particles emitted by ^{239,240}Pu and ^{238}Pu sorbed in the membrane was recorded and compared with that of an α source prepared on a stainless steel planchet with the same amount of Pu loaded in the HEMP-*co*-AMPS-grafted PES membrane sample. The two α spectra obtained are shown in Figure 2.

A comparison of the spectra given in Figure 2 suggests that the α energy spectrum recorded from the membrane sample is comparable to that obtained from the drop-deposited stainless steel planchet source. The left-side tailing of the α energy peaks is due to the 1−2 μm thickness of the bifunctional polymer, which would degrade the energy of the α-particles originating from the interior polymer matrix. The EDS line scan across thicknesses of the HEMP-*co*-AMPS-grafted membrane showed that P was distributed within 1−2 μm distance from the surface. However, the energy peak of α-particles emitted by ^{239,240}Pu (5.157−5.168 MeV) is well separated from that of α-particles emitted by ^{238}Pu (5.499 MeV), indicating the possibility of using ^{238}Pu as a tracer for quantifying ^{239}Pu in the unknown samples using the isotope dilution method.[40]

Sorption Efficiency and Chemical Selectivity. The sorption efficiencies of HEMP, AMPS, and HEMP-*co*-AMPS polymers toward Pu(IV) and Am(III) ions from aqueous solution were studied as a function of the HNO_3 concentration. As can be seen from Figure 3, the sorption efficiency of Pu(IV) in the HEMP polymer and HEMP-*co*-AMPS disks increased with increasing HNO_3 concentration in the equilibrating solution, and reached 60 ± 2% and 85 ± 3% at 3−4 mol L^{-1} HNO_3 in HEMP and HEMP-*co*-AMPS disks, respectively. The Am(III) sorption profile followed a reverse trend; i.e., the sorption efficiency decreased with increasing HNO_3 concentration. At any given HNO_3 concentration, the HEMP-*co*-AMPS disk showed better sorption efficiencies for both Pu(IV) and Am(III) than the pure HEMP disk. Two important conclusions that can be drawn from Figure 3 are (i) Pu(IV) can be discriminated from Am(III) representing a trivalent actinide at 3−4 mol L^{-1} HNO_3 concentration normally encountered in the nuclear fuel reprocessing plants or leach liquors and (ii) the Pu(IV) sorption efficiency of the HEMP-*co*-AMPS disk is significantly better than that of the pure HEMP disk.

The better Pu(IV) sorption efficiency of the HEMP-*co*-AMPS polymer could be attributed to the fact that AMPS provides anionic sites for a partial charge neutralization of Pu(IV) ions. It may also be possible that the presence of sulfate groups reduces the covalency in binding of Pu(IV) ions, which may enhance transfer of Pu(IV) ions from one binding site to another. This is important as the porosity of the disk is not sufficient to provide a high accessibility of the binding sites to Pu(IV) ions in an equilibrating solution. The increase of

dx.doi.org/10.1021/ac501509t | Anal. Chem. 2014, 86, 6254−6261

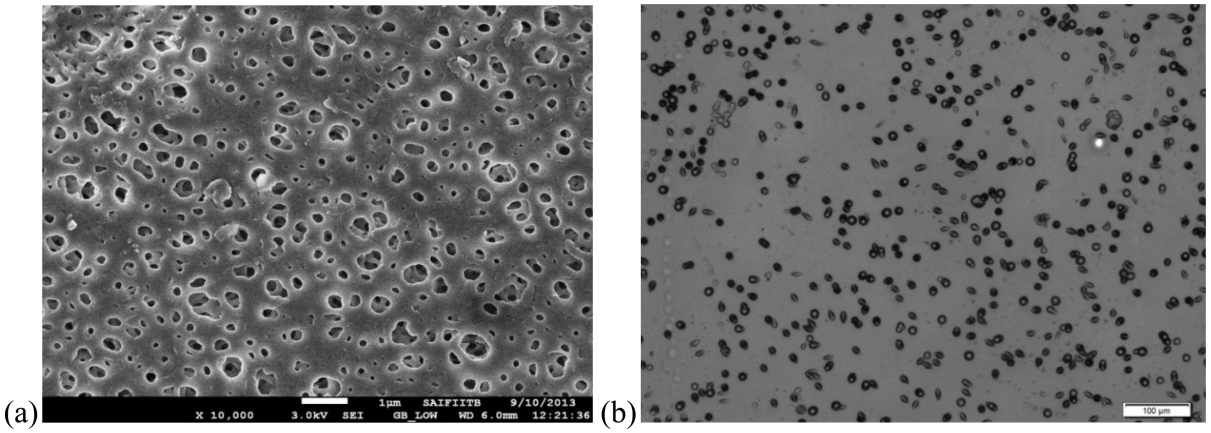

Figure 1. FE-SEM images of the grafted PES membrane (a) and α tracks in the CR-39 detector exposed to the Pu-loaded PES membrane (b).

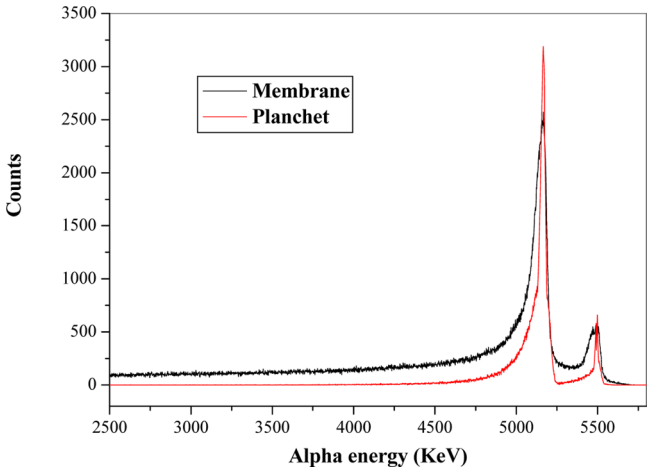

Figure 2. Comparison of the peak shapes obtained by α spectrometry of the Pu-loaded HEMP-*co*-AMPS-grafted PES membrane and Pu deposited on a stainless steel planchet. Both samples have equivalent amounts of Pu and are counted for the same time under identical geometrical conditions.

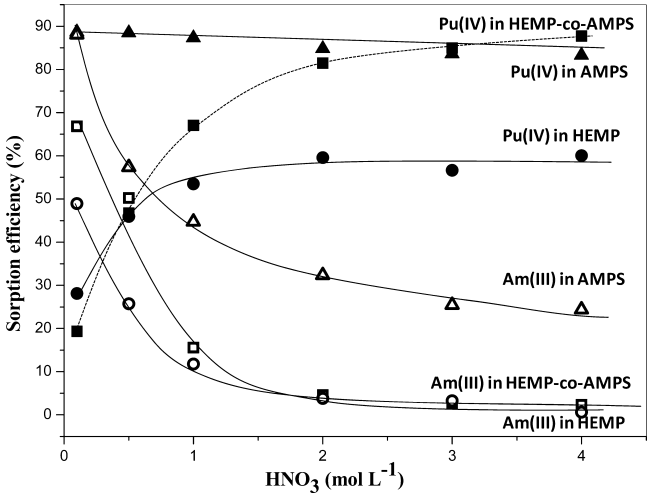

Figure 3. Sorption profiles of Am(III) and Pu(IV) in the HEMP (○), AMPS (△), and HEMP-*co*-AMPS (□) disks as a function of the HNO_3 concentration. Filled and unfilled symbols denote Pu(IV) and Am(III), respectively. Lines are drawn to guide the eyes.

Pu(IV) sorption efficiency with increasing HNO_3 concentration could be attributed to Pu(IV) complexation with neutral phosphate binding sites that require sorption of nitrate ions for charge balance in spite of the presence of sulfonic acid groups within the polymer matrix. The fixed −ve binding sites ($-SO_3^-$) would partially neutralize the +ve charges on Pu(IV) ions due to a geometrical constraint on the cross-linked polymer matrix. The decrease in Am(III) sorption efficiency with increasing HNO_3 concentration seems to suggest that an ion-exchange mechanism plays a dominant role in Am sorption. The presence of 25% diester in the HEMP monomer is responsible for the ion-exchange mechanism in the pure HEMP disk.

To understand the role of AMPS, Pu(IV) and Am(III) sorptions in the AMPS disks were studied as a function of the HNO_3 concentration in an equilibrating solution. The Am(III) sorption efficiency in the AMPS disk decreased with the HNO_3 concentration, which was similar to the Am(III) sorption profiles in the HEMP and HEMP-*co*-AMPS disks. However, it is seen from Figure 3 that the Am sorption efficiency in the AMPS disk is better than that in the HEMP and HEMP-*co*-AMPS disks. For example, the Am(III) sorption efficiency in the AMPS disk is 30% at 3−4 mol L^{-1} HNO_3, while Am(III) sorption is negligible in the HEMP and HEMP-*co*-AMPS disks under similar conditions. Thus, Pu(IV) and Am(III) discrimination is better in the HEMP-*co*-AMPS disk as compared to the AMPS disk.

The Pu(IV) sorption efficiency in the AMPS disk did not vary with the HNO_3 concentration but remained constant at 87 ± 3%. The AMPS disk contains sulfonic acid groups which are not selective for Pu(IV) in the presence of competing actinide ions with higher oxidation states such as U(VI). Therefore, the distribution coefficients of Pu(IV) (D_{Pu}) and U(VI) (D_U) were measured in the presence of both the ions. As can be seen from Table 2, the ratio of D_{Pu} to D_U is much higher (84.29) in the

Table 2. Comparison of the Distribution Coefficients of Pu(IV) and U(VI) in the AMPS and HEMP-*co*-AMPS Disks in the Presence of Both Ions[a]

polymer sample	D_U (mL g^{-1})	D_{Pu} (mL g^{-1})	D_{Pu}/D_U
AMPS	0.64	2.21	3.44
HEMP-*co*-AMPS	0.04	3.37	84.29

[a]The concentration of U(VI) was 5 times greater than that of Pu(IV) in equilibrating 3 mol L^{-1} HNO_3.

dx.doi.org/10.1021/ac501509t | *Anal. Chem.* 2014, 86, 6254−6261

Table 3. Comparison of the Isotopic Composition of Pu Determined by Single-HEMP-*co*-AMPS-Bead-Based TIMS with that Obtained by Solution-Based TIMS

	sample 1 concn (atom %)		sample 2 concn (atom %)	
isotope	HEMP-*co*-AMPS bead[a]	solution	HEMP-*co*-AMPS bead[a]	solution
^{239}Pu	68.82 ± 0.04	68.79 ± 0.03	68.55 ± 0.04	68.58 ± 0.03
^{240}Pu	26.95 ± 0.012	26.94 ± 0.03	27.23 ± 0.08	27.25 ± 0.03
^{241}Pu	2.06 ± 0.006	2.09 ± 0.006	1.95 ± 0.007	1.93 ± 0.006
^{242}Pu	2.01 ± 0.008	2.02 ± 0.006	2.11 ± 0.015	2.10 ± 0.006

[a]Values are the average of four determinations.

HEMP-*co*-AMPS disk than that in the AMPS disk (3.44). This seems to suggest that Pu(IV) can be selectively sorbed in the HEMP-*co*-AMPS disk in the presence of competing ions such as U(VI).

Sorption Kinetics. To understand the role of sulfate groups in the transfer of Pu(IV) ions from the surface of the HEMP-*co*-AMPS disk to its interior matrix, the Pu(IV) sorption rate kinetics was studied. The Pu(IV) sorption rate profile from 2 mol L^{-1} HNO_3 is shown in Figure S5 (Supporting Information). The choice of a high HNO_3 concentration was to avoid Pu hydrolysis and polymerization, and also at 2 mol L^{-1} HNO_3 concentration, the ion-exchange mechanism would not have a major effect on the sorption rate profile. It is seen from Figure S5a that the initial sorption of Pu(IV) is very fast; i.e., 50% attainment of Pu(IV) sorption equilibrium occurred in 5 min of equilibration time. Thereafter, sorption becomes slow, which could be attributed to slow transfer of Pu(IV) ions from the surface of the HEMP-*co*-AMPS disk to its interior matrix. In the case of the pure HEMP, the Pu sorption efficiency did not increase beyond 60% due to strong binding of Pu(IV), which would hinder transfer of Pu(IV) ions from the surface to the interior matrix. The sorption rate profile, beyond 5 min of equilibration time, could be fitted to the linearized pseudo-second-order rate equation given below, which is normally observed in chemical sorption of ions in the sorbent at the tracer concentration:[41]

$$\frac{t}{q_t} = \frac{1}{K_2 q_e^{\,2}} + \frac{t}{q_e} \tag{4}$$

where q_t and q_e are the amounts of solute sorbed per unit weight of the sorbent at time t and at equilibrium, respectively, and K_2 is the pseudo-second-order rate constant of sorption. The value of q_e deduced from the slope of the fitted Pu sorption rate profile in the HEMP-*co*-AMPS disk with eq 4 was found to be 107 μg of Pu g^{-1}, which is in good agreement with the experimentally measured Pu loading capacity 108 μg of Pu g^{-1}. The value of the pseudo-second-order rate constant (K_2) was found to be 0.95 g μmol^{-1} s^{-1}.

Reusability. Desorption of actinide ions is important for the reusability of the bifunctional polymer. The desorption of trivalent actinides such as Am(III) is possible from the HEMP and HEMP-*co*-AMPS disks with a high HNO_3 concentration as indicated in the Am(III) sorption profile shown in Figure 3. Pu(IV) desorption was found to be possible to an extent of 80% from the HEMP-*co*-AMPS disk by single equilibration in 1 mol L^{-1} $NH_2OH{\cdot}HCl$ overnight. This was attributed to the reduction of Pu(IV) to Pu(III) by hydroxylamine hydrochloride. However, Pu(IV) could be deloaded only 40% from the HEMP disk with 1 mol L^{-1} $NH_2OH{\cdot}HCl$. This indicated that the presence of sulfonic acid groups in the HEMP-*co*-AMPS disk not only improved the sorption properties of the disk but also enhanced the desorption of Pu(IV). After desorption, Pu(IV) could again be loaded with the same efficiency, suggesting its reusability.

Analytical Applications. Pu isotopic analyses of the PHWR grade Pu were carried out by subjecting a single bead of the HEMP-*co*-AMPS polymer directly to TIMS as described in the Experimental Section. Pu(IV) was loaded into a HEMP-*co*-AMPS bead from a solution with 3 mol L^{-1} HNO_3 and a large excess of uranium (Pu/U weight ratio ~1/250). During TIMS analyses, no U^+ ions were observed. This was attributed to higher selectivity of the HEMP-*co*-AMPS polymer toward plutonium in nitric acid medium when Pu(IV) is present to saturate the binding sites. For comparison, the solution-based TIMS analysis was also carried out after removal of Am(III) and U(VI) by a conventional ion-exchange method described in the Experimental Section. It is seen from the data given in Table 3 that single-bead TIMS provides the isotopic composition of Pu with a reasonably good accuracy. Thus, a single HEMP-*co*-AMPS bead could be used for preconcentration, purification without involving a multistep and time-consuming ion-exchange column-based method, and isotopic composition analyses of Pu by its direct loading into the TIMS instrument. It is advantageous to use a single bead in TIMS as it is a point source reservoir for Pu ions that improves the ion optics of the TIMS instrument, resulting in a better ion collection efficiency. This has immense importance in handling of high-dose samples for Pu isotopic composition analyses.

The quantification of Pu(IV) in the aqueous samples was carried out using the HEMP-*co*-AMPS-grafted PES membrane using α spectrometry. The variation of the α counts in the membrane sample (2 × 1 cm^2) with the amount of Pu present in the membrane sample was found to be linear as shown in Figure S6 (Supporting Information). This was attributed to a fairly constant Pu(IV) sorption efficiency and highly reproducible geometry of the HEMP-*co*-AMPS membrane samples. A series of aqueous solutions with volumes in the range of 5−100 mL were spiked with the same amount of Pu tracer, and each solution was equilibrated with a 2 × 1 cm^2 piece of the HEMP-*co*-AMPS membrane. It was observed that the efficiency of preconcentration was nearly constant when the volume of the equilibrating solution was varied from 5 to 100 mL. However, a 100 mL volume requires 24 h of equilibration as compared to 1 h of equilibration of the membrane sample for 5−30 mL samples under constant stirring conditions.

To quantify Pu(IV) preconcentrated in the membrane samples, the absolute counting efficiency (α count rate/disintegration rate × 100) is required for a fixed geometry of sample in the counting chamber of the α spectrometer. Since the size of the membrane sample is not a point source, a large surface area detector (450 mm^2) was used for α counting. The absolute counting efficiencies for the 2 × 1 cm^2 membrane, 1 ×

dx.doi.org/10.1021/ac501509t | Anal. Chem. 2014, 86, 6254−6261

Table 4. Determinations of the Pu Concentration in Aqueous Samples by Membrane-Based α Spectrometry

		concn of Pu spiked		concn of Pu measured[c]	
sample[a]	sample vol (mL)	Bq mL^{-1}	ppb[b]	Bq mL^{-1}	ppb[b]
synthetic urine	5	20	4.11	20.2 ± 1.0	4.16 ± 0.21
seawater	5	15	3.08	14.9 ± 0.9	3.06 ± 0.18
	100	0.06	0.012	0.054 ± 0.004	0.011 ± 0.001
groundwater	30	0.32	0.067	0.31 ± 0.02	0.065 ± 0.004
soil leach liquor	100	0.11	0.022	0.092 ± 0.009	0.019 ± 0.002

[a]The HNO_3 concentration in all the samples was 3 mol L^{-1} except for the soil leach liquor. The HNO_3 concentration in the soil leach liquor was 8 mol L^{-1}. The amount of Pu spiked in the soil was 1.1 pg g^{-1}. [b]Based on a Pu specific α activity of 4.87 Bq pg^{-1} calculated from the isotopic composition. [c]Corrected for the sorption efficiency (85 ± 2% for 3 mol L^{-1} HNO_3 and 70 ± 2% for 8 mol L^{-1} HNO_3), which was determined using the appropriate sample volume and equilibration time.

1 cm^2 membrane, and plancheted point source sample were found to be 14.8%, 27.9%, and 29.7%, respectively. Thus, the absolute α counting efficiency of the 1 × 1 cm^2 membrane sample is comparable with that of the plancheted source and could be used for quantification of preconcentrated Pu(IV) in its matrix without affecting the count rate significantly.

Membrane-based α spectrometry was applied for the quantitative determinations of Pu in the synthetic urine sample with the composition given in the literature,[42] groundwater, seawater, and soil leach liquor. For determination of the sub parts per billion level (0.01 ppb) of Pu(IV), the 100 mL sample was equilibrated with the HEMP-*co*-AMPS membrane for 24 h. The α count rate obtained in the membrane sample was 0.034 counts s^{-1}, and 24 h of counting was required to accumulate sufficient counts above the background. The Pu content in the soil sample was determined by equilibrating the membrane sample to the soil leach liquor without adjusting the acidity. However, the extraction efficiency decreased from 85 ± 2% in 3 mol L^{-1} HNO_3 to 70 ± 2% in 8 mol L^{-1} HNO_3. The data given in Table 4 seem to suggest that HEMP-*co*-AMPS-membrane-based α spectrometry offers good precision and accuracy for quantifying sub parts per billion amounts of Pu(IV) in complex environmental samples. However, the membrane-based isotope dilution technique would be better to avoid possible errors caused by a variation in the dimensions of the membrane, a change in the counting efficiency, an inefficient conversion of the Pu oxidation state to Pu(IV), and an unknown chemical composition of a solution. The present method can be easily adopted as the isotope dilution technique.

CONCLUSIONS

The bifunctional HEMP-*co*-AMPS polymer was found to have a better Pu(IV) sorption efficiency than the HEMP polymer and a better ability to discriminate Pu(IV) from Am(III) than the AMPS polymer in 3−4 mol L^{-1} HNO_3. The bifunctional HEMP-*co*-AMPS was found to sorb Pu(IV) selectively in the presence of a large excess of U(VI) ions. This bifunctional polymer could be made as a self-supporting disk or anchored as a 1−2 μm thin film on the poly(ether sulfone) membrane. Single-HEMP-*co*-AMPS-bead-based TIMS was used for determination of the isotopic composition of PHWR grade Pu in 3−4 mol L^{-1} HNO_3 with minimal sample manipulation and reasonably good accuracy. Use of a single-bead loading also improved the ion collection efficiency in the TIMS instrument. HEMP-*co*-AMPS grafted onto the PES membrane was found to be effective for the preconcentration of Pu(IV) from a high HNO_3 concentration, normally encountered in nuclear fuel reprocessing plant waste streams and leach liquors of geological and biological objects, and subsequent quantification with α spectrometry. Also, secondary waste generated could be minimized since the HEMP-*co*-AMPS-grafted membranes can be regenerated and reused.

ASSOCIATED CONTENT

Supporting Information

Table listing the isotopic composition of the Pu stock solution used in the present study and figures showing the chemical structures of HEMP and AMPS used in the preparation of the bifunctional polymer, the Teflon mould used for UV polymerization to form bifunctional polymer disks, formation of free radicals on the surface of a poly(ether sulfone) membrane on exposure to UV light, elemental analysis of the HEMP-*co*-AMPS polymer and HEMP-*co*-AMPS-grafted PES membrane by EDS, attainment of sorption equilibrium $[F(t)]$ as a function of the equilibration time t of the HEMP-*co*-AMPS disk in a well-stirred solution containing Pu(IV) in 2 mol L^{-1} HNO_3, a profile fitted with the pseudo-second-order rate kinetics equation, and variations of α activity obtained by α spectrometry of the Pu(IV)-loaded HEMP-*co*-AMPS membrane as a function of the amount of Pu(IV) in the membrane. This material is available free of charge via the Internet at http://pubs.acs.org.

AUTHOR INFORMATION

Corresponding Author

*Phone: +91-22-25593740. Fax: +91-22-25505150/25505151. E-mail: skaggr@barc.gov.in; skaggr2002@gmail.com.

Notes

The authors declare no competing financial interest.

REFERENCES

(1) Gavrilescu, M.; Pavel, L. V.; Cretescu, I. *J. Hazard. Mater.* **2009**, *163*, 475−510.
(2) Gorden, A. E. V.; Xu, Jide; Raymond, K. N.; Durbin, P. *Chem. Rev.* **2003**, *103*, 4207−4282.
(3) Schwantes, J. M.; Orton, C. R.; Clark, R. A. *Environ. Sci. Technol.* **2012**, *46*, 8621−8627.
(4) Zolotov, Y. A.; Tsysin, G. I.; Morosanova, E. I.; Dmitrienko, S. G. *Russ. Chem. Rev.* **2005**, *74*, 37−60.
(5) Guérin, N.; Calmette, R.; Johnson, T.; Larivière, D. *Anal. Methods* **2011**, *3*, 1560−1567.
(6) Kumar, S. A.; Pandey, S. P.; Thakur, N.; Parab, H.; Shinde, R. N.; Pandey, A. K.; Wagh, D. N.; Kumar, S. D.; Reddy, A. V. R. *J. Hazard. Mater.* **2013**, *262*, 265−273.
(7) Milliard, A.; Durand-Jézéquel, M.; Larivière, D. *Anal. Chim. Acta* **2011**, *684*, 40−46.
(8) Kim, G.; Burnett, W. C.; Horwitz, E. P. *Anal. Chem.* **2000**, *72*, 4882−4887.

(9) Mekki, S.; Bouvier-Capely, C.; Jalouali, R.; Rebière, F. *Radiat. Prot. Dosim.* **2011**, *144*, 330−334.
(10) Chavan, V.; Paul, S.; Pandey, A. K.; Kalsi, P. C.; Goswami, A. *J. Hazard. Mater.* **2013**, *260*, 53−60.
(11) Lebed, P. J.; Savoie, J.-D.; Florek, J.; Bilodeau, F.; Larivière, D.; Kleitz, F. *Chem. Mater.* **2012**, *24*, 4166−4176.
(12) Lebed, P. J.; de Souza, K.; Florek, J.; Bilodeau, F.; Larivière, D.; Kleitz, F. *Chem. Commun.* **2011**, *47*, 11525−11527.
(13) Manos, M. J.; Kanatzidis, M. G. *J. Am. Chem. Soc.* **2012**, *134*, 16441−16446.
(14) Sun, Y.; Shao, D.; Chen, C.; Yang, S.; Wang, X. *Environ. Sci. Technol.* **2013**, *47*, 9904−9910.
(15) Vajda, N.; Kim, C.-K. *Anal. Chem.* **2011**, *83*, 4688−4719.
(16) Bai, F.; Ye, G.; Chen, G.; Wei, J.; Wang, J.; Chen, J. *React. Funct. Polym.* **2013**, *73*, 228−236.
(17) Fryxell, G. E.; Lin, Y.; Fiskum, S. K.; Birnbaum, J. C.; Wu, H. *Environ. Sci. Technol.* **2005**, *39*, 1324−1331.
(18) Lin, Y.; Fiskum, S. K.; Yantasee, W.; Wu, H.; Mattigod, S. V.; Vorpagel, E.; Fryxell, G. E.; Raymond, K. N.; Xu, J. *Environ. Sci. Technol.* **2005**, *39*, 1332−1337.
(19) Birnbaum, J. C.; Busche, B.; Lin, Y.; Shaw, W. J.; Fryxell, G. E. *Chem. Commun.* **2002**, 1374−1375.
(20) Johnson, A. K.; Kaczor, J.; Han, H.; Kaur, M.; Tian, G.; Rao, L.; Qiang, Y.; Paszczynski, A. J. *J. Nanopart. Res.* **2011**, *13*, 4881−4895.
(21) Nuňz, L.; Kaminski, M. D. *J. Magn. Magn. Mater.* **1999**, *194*, 102−107.
(22) Ebner, A. D.; Ritter, J. A.; Navratil, J. D. *Ind. Eng. Chem. Res.* **2001**, *40*, 1615−1623.
(23) Matthews, S. E.; Parzuchowski, P.; Garcia-Carrera, A.; Grüttner, C.; Dozol, J.-F.; Böhmer, V. *Chem. Commun.* **2001**, 417−418.
(24) Grüttner, C.; Böhmer, V.; Casnati, A.; Dozol, J.-F.; Reinhoudt, D. N.; Reinoso-Garcia, M. M.; Rudershausen, S.; Teller, J.; Ungaro, R.; Verboom, W.; Wang, P. *J. Magn. Magn. Mater.* **2005**, *293*, 559−566.
(25) Kaur, M.; Johnson, A.; Tian, G.; Jiang, W.; Rao, L.; Paszczynski, A.; Qiang, Y. *Nano Energy* **2013**, *2*, 124−132.
(26) Vajda, N.; Törvényi, A.; Kis-Benedek, G.; Kim, C. K.; Bene, B.; Mácsik, Zs. *Radiochim. Acta* **2009**, *97*, 395−401.
(27) Eikenberg, J.; Jäggi, M.; Beer, H.; Rüthi, M.; Zumsteg, I. *Appl. Radiat. Isot.* **2009**, *67*, 776−780.
(28) Thakur, P.; Mulholland, G. P. *J. Radioanal. Nucl. Chem.* **2011**, *288*, 499−506.
(29) Larivière, D.; Benkhedda, K.; Kiser, S.; Johnson, S.; Cornett, R. J. *Anal. Methods* **2010**, *2*, 259−267.
(30) Grate, J. W.; O'Hara, M. J.; Farawila, A. F.; Douglas, M.; Haney, M. M.; Petersen, S. L.; Maiti, T. C.; Aardahl, C. L. *Anal. Chem.* **2011**, *83*, 9086−9091.
(31) Labrecque, C.; Whitty-Léveillé, L.; Lariviré, D. *Anal. Chem.* **2013**, *85*, 10549−10555.
(32) Qiao, J.; Hou, X.; Roos, P.; Miro, M. *Anal. Chem.* **2013**, *85*, 2853−2859.
(33) Alexandratos, S. D.; Hussain, L. A. *Ind. Eng. Chem. Res.* **1995**, *34*, 251−254.
(34) (a) Yamagishi, H.; Crivello, J. V.; Belfort, G. *J. Membr. Sci.* **1995**, *105*, 237−247. (b) Rivaton, A.; Gardette, J. L. *Polym. Degrad. Stab.* **1999**, *66*, 385−403. (c) Akbari, A.; Desclaux, S.; Rouch, J. C.; Aptel, P.; Remigy, J. C. *J. Membr. Sci.* **2006**, *286*, 342−350.
(35) (a) Paul, S.; Sarkar, A.; Alamelu, D.; Shah, R. V.; Aggarwal, S. K. *Radiochim. Acta* **2012**, *100*, 291−296. (b) Ramaniah, M. V.; Jain, H. C.; Aggarwal, S. K.; Chitambar, S. A.; Kavimandan, V. D.; Almaula, A. I.; Shah, P. M.; Parab, A. R.; Sant, V. L. *Nucl. Technol.* **1980**, *49*, 121−128.
(36) (a) Das, S.; Pandey, A. K.; Athawale, A. A.; Manchanda, V. K. *Ind. Eng. Chem. Res.* **2009**, *48*, 6789−6796. (b) Vasudevan, T.; Das, S.; Sodaye, S.; Pandey, A. K.; Reddy, A. V. R. *Talanta* **2009**, *78*, 171−177. (c) Vasudevan, T.; Pandey, A. K.; Das, S.; Pujari, P. K. *Chem. Eng. J.* **2014**, *236*, 9−16.
(37) Pandey, A. K.; Sharma, R. C.; Kalsi, P. C.; Iyer, R. H. *Nucl. Instrum. Methods Phys. Res., B* **1993**, *82*, 151−155.
(38) Clark, D. L.; Hecker, S. S.; Jarvinen, G. D.; Neu, M. P. Plutonium. *The Chemistry of the Actinide and Transactinide Elements*; Springer: Dordrecht, The Netherlands, 2006.
(39) Batueva, T. D.; Gorbunova, M. N.; Scherban, M. G. *J. Appl. Polym. Sci.* **2013**, *129*, 1978−1984.
(40) Joe, K.; Han, S.-H.; Song, B.-C.; Lee, C.-H.; Ha, Y.-K.; Song, K. *Nucl. Eng. Technol.* **2013**, *45*, 415−420.
(41) Das, S.; Pandey, A. K.; Athawale, A. A.; Manchanda, V. K. *J. Phys. Chem. B* **2009**, *113*, 6329−6335 and references therein.
(42) McCurdy, D.; Lin, Z.; Inn, K. G. W.; Bell, R., III; Wagner, S.; Efurd, D. W.; Steiner, R.; Duffy, C.; Hamilton, T. F.; Brown, T. A.; Marchetti, A. A. *J. Radioanal. Nucl. Chem.* **2005**, *263*, 447−455.